Article

Optimizing Building Thermal Insulation: The Impact of Brick Geometry and Thermal Coefficient on Energy Efficiency and Comfort

Ioannis Makrygiannis [1,]* and **Konstantinos Karalis** [2]

1   SABO Clay Laboratory and Research Department, SABO S.A., 34002 Vasiliko, Greece
2   Institute of Geological Sciences, University of Bern, CH-3012 Bern, Switzerland;
    konstantinos.karalis@geo.unibe.ch
*   Correspondence: ymakrigiannis@sabo.gr

Abstract: The thermal insulation properties of building walls are critical to the overall energy efficiency and comfort of a building. One important factor that can affect these properties is the type of bricks used in construction. Bricks can vary in their geometry and thermal coefficient, which can impact their ability to transfer heat through the wall. The geometry of a brick can affect its thermal properties by altering the amount of air trapped within it and the surface area available for heat transfer. Hollow bricks or those with complex geometries may have lower thermal conductivity than regular solid bricks due to the air pockets trapped within them. Conversely, larger surface areas on the exterior of the brick can increase heat transfer. The thermal coefficient of clay, a common material used in brick production, is another important factor. Clay has relatively low thermal conductivity, meaning it is a poor conductor of heat. However, the quality of the clay, as well as the firing temperature and duration used in brick production, can impact its thermal coefficient. Higher firing temperatures and longer firing times can result in a more compact and dense clay brick, which can improve its thermal properties. In summary, the thermal insulation properties of building walls can be significantly affected by the type of bricks used in their construction. It is important to consider the geometry and thermal coefficient of the bricks when designing a building to achieve the desired level of thermal insulation. By selecting bricks with appropriate properties, designers can help to improve the energy efficiency and comfort of the building while reducing its environmental impact.

Keywords: thermal insulation; energy efficiency; environmental impact

1. Introduction

The use of bricks in construction has a long history dating back to ancient civilizations [1]. Over time, the manufacturing process of bricks has evolved, leading to the development of new and improved materials. In recent years, Computational Fluid Dynamics (CFD) software has become an invaluable tool for studying the thermal behavior of materials, including bricks. This has opened up new avenues for research and development in the field of construction materials.

The thermal insulation properties of a building wall can be affected by the type of bricks used in its construction. Bricks can vary in their thermal conductivity, which is a measure of how easily heat flows through the material [2]. For example, solid bricks made of dense materials like concrete or clay have a higher thermal conductivity than hollow bricks made of lightweight materials like clay, cement, or pumice. This means that solid bricks will transfer more heat through the wall, resulting in higher energy costs for heating and cooling the building.

On the other hand, hollow bricks with air pockets inside provide a layer of insulation and can reduce heat transfer through the wall. The air pockets act as a barrier to the

transfer of heat, which can help to keep the building cooler in the summer and warmer in the winter [3].

Clay bricks have a relatively low thermal conductivity due to the low thermal coefficient of clay, which means they are good insulators. However, the thermal conductivity of a clay brick can be further reduced by incorporating insulating materials such as perlite or vermiculite into the clay mixture during production. These materials create air pockets within the brick, which provide additional insulation and reduce heat transfer through the wall [4].

In addition to the type of bricks used, the thickness and composition of the mortar between the bricks can also affect the thermal insulation properties of the wall. If the mortar is too thin or does not bond well with the bricks, it can create gaps that allow heat to escape or enter the building. Choosing the right type of brick and mortar for a building wall can have a significant impact on its thermal insulation properties and, ultimately, on the energy efficiency and comfort of the building [5].

Plaster can also play an important role in the thermal insulation of buildings. When applied properly, plaster can help to improve the thermal performance of a wall by reducing heat transfer through the wall. One of the main ways that plaster can improve thermal insulation is by filling in gaps and imperfections in the wall surface. These gaps and imperfections can create areas where heat can escape or enter the building. By applying a layer of plaster over the wall surface, these gaps and imperfections can be filled, creating a more uniform surface that reduces heat transfer [6].

In this article, the thermal behavior of a traditional Greek brick and a new different type of brick will be compared using CFD software. Specifically, (i) the geometry of the bricks and (ii) the impact of the thermal coefficient of fired material on the thermal behavior of the bricks will be explored. This parameter, which varies depending on the manufacturing process, has a significant influence on the heat transfer properties of the bricks, which in turn affects their thermal performance in construction applications.

The primary objective of this study was to examine the effect of the thermal coefficient on fired materials by constructing and analyzing two different clay mixtures. The first mixture comprised argile clay material, while the second and third mixtures incorporated 2% and 8% of solid waste material, specifically paper sludge [7], respectively. The mixtures were prepared through extrusion, followed by drying and firing under laboratory conditions that simulated real brick industry production environments. Data on the density and thermal coefficient of the fired samples were collected and analyzed to evaluate their overall properties and understand the impact of geometric variations and waste additive inclusion on thermal insulation characteristics. This investigation aimed to provide valuable insights into optimizing the thermal insulation efficiency of bricks and their applications in building construction.

To achieve this objective, various geometric parameters were systematically altered, and the corresponding thermal insulation properties were measured. The study focused on understanding how changes in the brick's geometry, such as dimensions, shape, and surface patterns, affected its ability to prevent heat transfer [8]. Additionally, the research examined the effects of incorporating a waste additive into the brick manufacturing process, which resulted in a reduction in the final product's density [9]. The investigation aimed to determine the extent to which this density reduction influenced the thermal insulation properties of the bricks and the walls constructed using them.

By analyzing these critical factors, the study sought to provide valuable insights into optimizing the thermal insulation efficiency of bricks and their applications in building construction.

Table 1. The three (3) labeled constructed mixtures with the ratio of the additive in the mixture.

Mixture	TZ	TPS2	TPS8
	wt.%	wt.%	wt.%
Clay material TZ	100	98	92
Paper sludge	-	2	8

The aforementioned data (Table 1) on the thermal coefficient of the fired clay mixtures were utilized in the computational fluid dynamics (CFD) simulations to analyze the thermal performance of two actual bricks. The objective was to investigate the impact of the density and thermal coefficient of the clay on the thermal behavior of the bricks and their influence on the building's overall thermal performance.

By analyzing the thermal behavior of current perforated bricks and new types of bricks (vertical perforated clay blocks), insights can be gained into the advantages and disadvantages of each material, as well as identify areas for further research and development. Ultimately, this research has the potential to inform the selection of bricks for construction projects, leading to more efficient and sustainable building practices.

Traditionally, research in the field has predominantly focused on two distinct areas: the impact of brick geometry on the thermal behavior of buildings and the influence of waste additives on the physicochemical properties of fired bricks [10]. However, this study aims to bridge these two sectors of investigation by examining the combined effects of brick geometry and waste additives on thermal performance. By integrating these two previously separate areas of study, the research intends to provide a comprehensive understanding of how both factors interact and contribute to the overall thermal behavior and insulation properties of the bricks. This novel approach seeks to offer valuable insights into optimizing the design and production of bricks with enhanced thermal insulation capabilities, thereby advancing sustainable building practices.

2. Materials and Methods

2.1. Brick Products

Hollow bricks with horizontal holes are a type of clay brick that have one or more rows of continuous, horizontal holes running through the brick. These holes are typically located in the center of the brick and run parallel to the ground. This type of brick is the most common in the Greek market [11].

The purpose of the horizontal holes is to reduce the weight of the brick and provide better insulation. By creating hollow spaces within the brick, it becomes lighter and easier to handle during construction [12]. Additionally, the hollow spaces create a barrier that helps to prevent heat transfer, keeping the interior of a building cooler in the summer and warmer in the winter.

Hollow bricks with horizontal holes are commonly used in construction for both load-bearing and non-load-bearing walls. They are available in a variety of sizes and shapes, including standard rectangular bricks, corner bricks, and bricks with interlocking edges. Bricks can be used in a variety of applications, including residential, commercial, and industrial construction.

For the current study, the drawing of the most common constructing brick in the Greek market was provided by the company SABO S.A. for the purpose of the tests. The dimensions of the brick are 120 × 90 × 190 mm (Height × Width × Length) and can be seen in Figure 1.
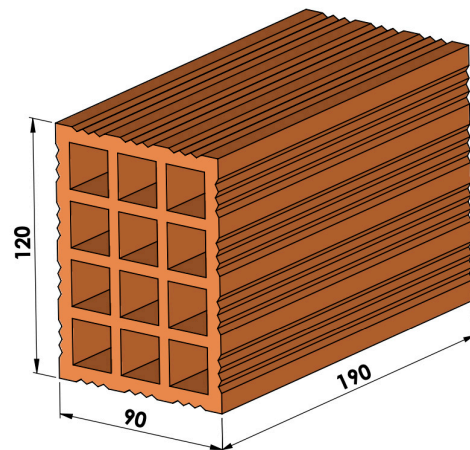
Figure 1. Most common hollow brick in the Greek market with horizontal hollows.

Vertically perforated bricks are a type of clay brick that have one or more vertical perforations running through the center of the brick. These perforations are typically circular or rectangular in shape and run from top to bottom rather than horizontally, like the holes in hollow bricks with horizontal holes [13].

The vertical perforations in the bricks create a larger surface area, which allows for more air circulation and, therefore, better insulation. As mentioned earlier, hot air rises and cold air sinks, so the vertical perforations allow for natural convection currents to be established within the walls. This helps to keep the interior of the building cooler in the summer and warmer in the winter [14].

Vertically perforated bricks are available in a variety of sizes and shapes, including standard rectangular bricks, corner bricks, and bricks with interlocking edges. They can be used in a variety of applications, including load-bearing and non-load-bearing walls, as well as for decorative purposes.

For the purpose of the study, a drawing of a new entry vertical clay block in the Greek market was provided by the SABO S.A. company. The dimensions of the brick were 240 × 250 × 250 mm (Height × Width × Length) and can be seen in the following Figure 2.
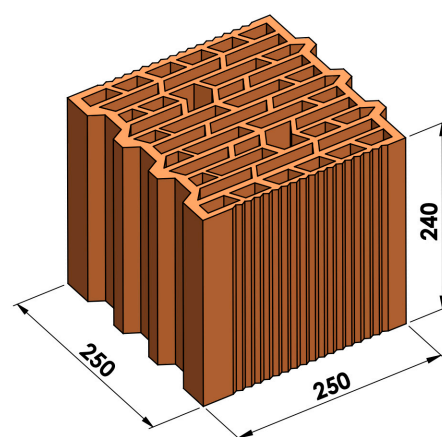

Figure 2. Vertically perforated brick in the Greek market.

2.2. Construction Mixture Components

2.2.1. Characteristics of Clay Material

The study utilized a typical type of clay commonly used in industrial brick production in the Evia region, which is referred to as TZ clay. According to ISO 14688-2:2017, TZ clay is an inorganic type with moderate plasticity, as its liquid limit falls within the range of 35–50%. Table 2 provides information on the properties of the clay. The chemical composi-

tion of the clay was determined through Atomic Absorption Spectrometry (AAS), following the ISO 26845:2016 standard, and is presented in Table 3.

The particle size of the clay was analyzed in accordance with ASTM D422-63 (2007), revealing a particle size range from 2 mm to 2 μm (Table 4). The clay was transported from the manufacturing site to the laboratory with an average humidity content of 8.15%, and its density was measured as 1781 Kg/m^3 on average, following the ASTM D698-12 standard.

Table 2. Physical properties of TZ clay.

Physical Properties	Unit	Values
Plastic limit	%	20.76
Liquid limit	%	42.00
Plasticity	%	24.23
Density	kg/m^3	1781

Table 3. Oxide composition of TZ clay.

Oxides (%)	SiO_2	Al_2O_3	CaO	Fe_2O_3	MgO	K_2O	Na_2O	LOI
TZ clay	56.45	16.72	5.65	5.08	2.73	1.64	0.55	9.34

Table 4. Particle size distribution of clay TZ.

Grain Size	Coarse Sand	Fine Sand	Silt	Clay
	>63 μm	63–20 μm	20 to 2 μm	<2 μm
TZ clay	6.00%	9.35%	40.37%	44.28%

2.2.2. Characteristics of Solid Waste Additive

The selected additive for solid waste to decrease its final density is paper sludge. Paper sludge is a byproduct of the paper-making process, and it is considered an industrial waste. It consists of various materials such as cellulose fibers, inorganic fillers, and additives used in the paper-making process [15].

In the past, paper sludge was often disposed of in landfills, which posed environmental problems, such as soil contamination and methane gas emissions. However, in recent years, there has been a growing interest in finding alternative uses for paper sludge to reduce waste and promote sustainability. One possible use for paper sludge is as a fuel source. It can be burned to generate energy, either alone or in combination with other fuels. Another option is to use paper sludge as a raw material in the production of other products such as bricks, cement, and fertilizer [16].

In addition, some researchers have investigated the potential use of paper sludge as a soil amendment due to its high organic content. However, there are concerns about potential contaminants in paper sludge, such as heavy metals, which may limit its use in this way [17].

Overall, while paper sludge is still considered an industrial waste, the use of this material can provide significant results on a brick mass. The addition of 8% paper sludge in a ceramic mass led to a decreased index of body density by 13.4%, and as a result of this fact, the thermal insulation coefficient was reduced by 17.3% [18].

Considering these outcomes, paper sludge was selected as one of the lightweight additives to be compared with other alternatives in the current research. The paper sludge used in this study was obtained from an Israeli brick and tile factory in the Beer Sheva region and had a humidity level of 65%. Determining the grain size accurately was challenging due to the high water [19] content in its mass. Therefore, the sludge was mixed thoroughly with the clay material TZ, which had a humidity level of 8.15%. As a result, the necessary mixing water was added to the paper sludge to achieve a homogenous mixture, which was stirred continuously for 24 h.

The chemical composition (wt.%) of the paper sludge was determined via X-ray fluorescence (XRF) and is presented in Table 5. The calcium oxide in paper sludge serves multiple purposes in brick production. It helps in the binding process by reacting with water and other components of the sludge, creating a cohesive mixture. Calcium hydroxide, which forms during hydration, acts as a cementitious material, contributing to the binding and hardening of the brick [20]. The reason why calcium oxide does not negatively affect the mechanical strength of the final product lies in the hydration process. During hydration, the calcium oxide absorbs water and undergoes a volume expansion. This expansion creates interlocking bonds between the particles, resulting in a stronger and more compact structure [21].

Table 5. Oxide composition of paper sludge.

Oxides (%)	SiO_2	Al_2O_3	CaO	Fe_2O_3	MgO	K_2O	Na_2O	C
Paper sludge	22.3	12.0	34.6	0.4	2.1	0.1	0.3	22.0

2.3. Methods

The research process involved obtaining clay material (TZ) which was ground and semi-wet prepared in the laboratory. The prepared clay was then extruded into solid specimens and subjected to an 8-step drying program lasting 24 h. The dried specimens were fired at a peak temperature of 900 °C using a 10-step firing program. Results were collected from this firing process. A second and a third mixture were then prepared, consisting of clay TZ with 2 and 8% paper sludge respectively, and subjected to the same testing procedure. Results were collected and compared between the three mixtures. All testing procedures were conducted in accordance with industrial-scale production for brick and tile industries. The aim of the research was to investigate the potential use of paper sludge as a raw material in the production of bricks and tiles. The Archimedes method based on ASTM C373-14a was used to determine the bulk density. The thermal conductivity (λ 10, dry, mat) of the fired clay samples was calculated according to EN1745:2012.

Following the calculation of the thermal coefficient of the fired brick samples, which were produced from two different mixtures, the thermal transmittance (U value) and thermal coefficient of the resulting brick drawings were determined. Based on these thermal results, the thermal performance of a building wall was calculated. Specifically, the U value and thermal coefficient of the brick samples were used to determine the heat transfer rate through the wall, which is a critical factor in assessing the energy efficiency and thermal comfort of a building. These calculations provide valuable insights into the potential use of the investigated brick and tile materials in the construction industry and their suitability for meeting thermal performance standards in building design and construction.

2.3.1. Calculation of Density and Thermal Coefficient of the Mixtures Preparation

In the initial phase of each composite formulation, the moisture content of the clay material or additive was determined as the first step. Moisture content represents the percentage of water present in a moist raw material or additive, where the quantity of water is expressed as a percentage of the weight of the wet material. For the determination of moisture, the sample was weighed into a laboratory vessel and subjected to drying in an electric dryer of type SCN/400/DG at 105 °C for a duration of 24 h. After attaining a constant weight, the sample was reweighed, and the weight of the laboratory vessel was subtracted from the total weight.

Prior to mixing, the materials were subjected to pre-crushing using a jaw hammer (model A92) with a jaw opening of 2 mm. The crushed materials were then passed through a laboratory roller mill of type Verdes 080, with an adjustable separation of 1.2 mm between the two cylinders. The paper sludge was mixed with the requisite extruding water and stirred for 24 h. The clay material in the mixture was weighed according to the mixing ratio,

taking into account their actual moisture content, and then homogenized in a kneading mixer, with the addition of necessary preparation water. The amount of water added was continued until a satisfactory plasticity index, as determined by Pfefferkorn's test, was achieved.

The Pfefferkorn plasticity method is based on the evaluation of the deformation of the sample due to the fall of the calibrated plate on the underlying test body, shaped by means of the ancillary shaping tool. The Pfefferkorn test comprises two reading scales, one measuring deformation in millimeters and the other determining the test body deformation based on the Pfefferkorn theory. For the present study, the Ceramic Instruments 01CI4540 Pfefferkorn plasticity tester was used, and the calculation method was followed [22]. The addition of water was a unique pre-mixture process that depended on the absorptivity of the clay material and the extrusion process to be employed for a given final product.

Extrusion

The homogenized mixture was extruded through vacuum-extruded rectangular samples of standard dimensions for all tested mixtures. The laboratory utilized a HANDLE KHS-Type: PZVM8b model extruder for this purpose. The wet material was placed in the feeding chamber, on top of which there was a porch for material input, following a pre-extruder mixer that included a screw mixer pushing the material through an air vacuum chamber to the extruder's output. The pressure was continuously monitored through a pressure gauge. The outer extruding part had interchangeable molds, which were used to produce the desired size and shape of the extruded products. All extruded samples were solid, without any hollow portions on their mass, and had a size of $120 \times 20 \times 20$ mm (L $\times$ W $\times$ H). The vacuum pressure was constant and uniform for all tested mixtures, measuring 0.8 kp/cm^2 [23]. The plasticity of both mixtures was determined according to the Pfefferkorn method and found to be 0.83 and 0.84, respectively, upon the addition of the necessary amount of water. A total of 30 samples were produced for the tests, with 15 samples being constructed for each mixture.

Drying

All extruded specimens were marked and subjected to a smooth drying process in the laboratory electric oven (type SCN/400/DG). The drying process consisted of three distinct phases: the humidity phase, the shrinkage phase, and the drying phase, each demanding specific attention as they may create different issues on the samples [24].

During the humidity phase, it is crucial to maintain high levels of ambient humidity in the dryer to keep the surface pores of the bricks open. This phase is the most critical during drying as cracks, deformations, or fragility of the bricks may occur.

In the shrinkage critical point phase, the drying shrinkage should be complete before the temperature rises rapidly to complete drying. The temperature rise should happen gradually in this phase to avoid cracking issues.

In the last phase, the target is to reduce the remaining body humidity in the bricks as much as possible. All regulations should follow this demand and adjust to the production mixture and its behavior.

The primary objective of the drying process is to keep the surface pores of the samples open at the beginning to facilitate the loss of humidity from the internal body. This phase is critical as in the second phase, during which the temperature rises and the humidity of the dryer drops, cracks, deformations, or fragility may occur.

Firing

The firing process was conducted using an electric gradient kiln of Nabertherm model GR1300/13, which was computer-controlled with 10 time-duration steps. The firing procedure was designed to ensure adequate preheating, firing at the maximum temperature, and cooling of the samples. The samples were held at the maximum peak temperature of 900 °C, which is an average temperature for the building brick and tile industry, for 3 h.

The preheating and cooling phases were executed smoothly, particularly near 573 °C, to prevent any issues resulting from quartz inversion [25].

The rate of temperature increase varied between 0.7 and 1.16 °C/min, depending on the firing zone and the programmed procedure. The firing process, from cold to cold, took 24 h.

The mixtures exhibited no problems during firing, and the samples were completely dried before being loaded into the kiln. The samples were placed in the dryer for 24 h at 105 °C.

2.3.2. Thermal Performance of Clay-Fired Bricks

The thermal performance of clay bricks can be modeled directly using computational fluid dynamics (CFD) simulations or using a simplified method based on EN 1745, EN ISO 10211:2007, and EN ISO 6946 standards. In CFD, the governing partial equations (in a differential form) are discretized (converted to algebraic form) in order to be solved using direct or iterative linear solvers [26].

For the convective motion, the momentum Equations corresponding to a fluid of variable density are written as:

$$\frac{\vartheta}{\vartheta t}\rho + \nabla \cdot (\rho u) = 0 \tag{1}$$

and

$$\frac{\vartheta}{\vartheta t}(\rho u) + \nabla \cdot (\rho u u) = -\nabla P + \nabla \cdot (\mu \nabla u) + \rho g \tag{2}$$

where u is the velocity vector field (m s^{-1}), ρ is the fluid density (kg m^{-3}), P is the pressure (Pa), and μ is the dynamic viscosity (Pa s).

The temperature field is described by the energy conservation Equation:

$$\rho C_P \frac{\vartheta T}{\vartheta t} + \left(\rho C_p u \cdot \nabla\right) T = \nabla \cdot (k \nabla T) \tag{3}$$

where T is the temperature (K), Cp is the heat capacity (J kg^{-1} K^{-1}), and k is the thermal conductivity (W m^{-1} K^{-1}).

The radiative heat transfer is given by the radiant heat flux:

$$Q = \sigma \left(T_{max}^4 - T_{min}^4\right) \tag{4}$$

where T is the temperature (K) and σ is the Stefan-Boltzmann constant.

In the second approach, which is based on standards, the main challenge lies in calculating the effective properties of air cavities, particularly in cases where they are non-rectangular. To overcome this difficulty, the non-rectangular cavities must first be transformed into rectangular ones, and then the equivalent thermal conductivity can be calculated using the convective heat transfer coefficient (ha) and the radiative heat transfer coefficient (hr) [27]. Table 6 presents the properties of clay and air that are considered homogeneous fluid continua.

Table 6. Properties of materials used in the computations.

Properties	Porous Clay	Air
Density TZ (kg/m^3)	1720	1.23
Density TPS2 (kg/m^3)	1663	1.23
Density TPS8 (kg/m^3)	1490	1.23
Heat Capacity (J/(kg·K))	1000	1008
Thermal Conductivity TZ (W/(m·K))	0.52	Geometry and Temperature Dependent
Thermal Conductivity TPS2 (W/(m·K))	0.49	Geometry and Temperature Dependent
Thermal Conductivity TPS8 (W/(m·K))	0.43	Geometry and Temperature Dependent

In Figures 3 and 4, the geometry of the ceramic products and the respective domains are portrayed. The ceramic product is insulated at the bottom and the top side.

In the left-side wall, corresponding to the external wall, a convective heat flux boundary condition was applied, with an external temperatur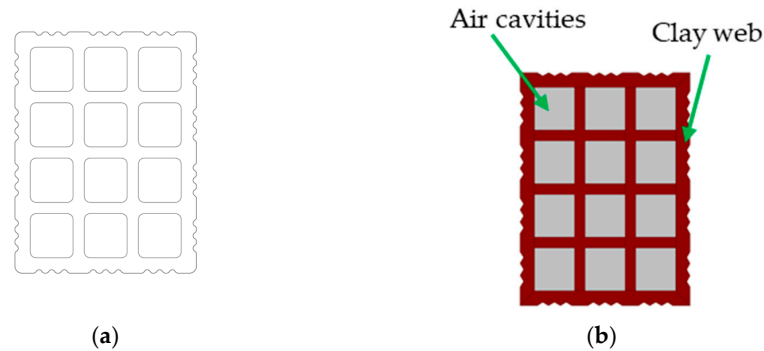e of 0 °C and a heat transfer coefficient of 25 W/(m^2·K). Similarly, in the right-side wall, corresponding to the inner wall, a convective heat flux boundary condition was applied, with a constant temperature of 20 °C and a heat transfer coefficient of 7.69 W/(m^2·K) [28].

(**a**)   (**b**)

Figure 3. (**a**) Ceramic geometry and (**b**) domains of horizontal hollows brick.

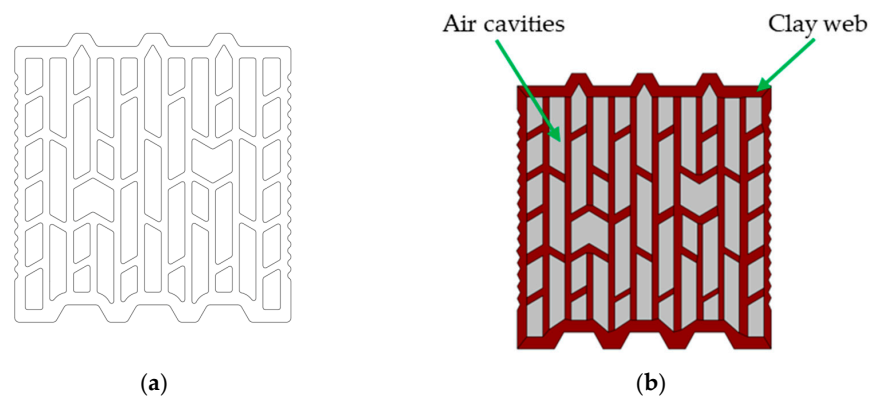(**a**)   (**b**)

Figure 4. (**a**) Ceramic geometry and (**b**) domains of vertically perforated brick.

Computational Details

Convergence was assumed when the scaled residuals of the discretized equations fell below a preset tolerance of 10^{-6}. The thermal problem was solved with the stationary direct solver PARDISO. The grid consisted of 73.864 triangular mesh elements (see Figures 5 and 6), with the lowest element quality being equal to 0.62 [29].
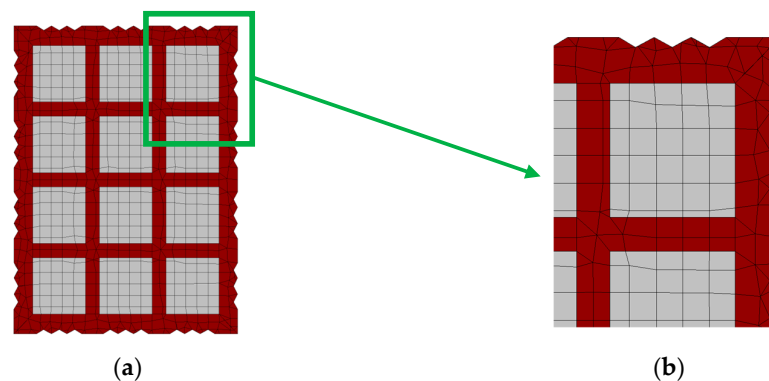

(**a**)   (**b**)

Figure 5. Schematic of the computational grid used for the brick with horizontal holes (**a**) in the ceramic products (**b**) around the air hole.
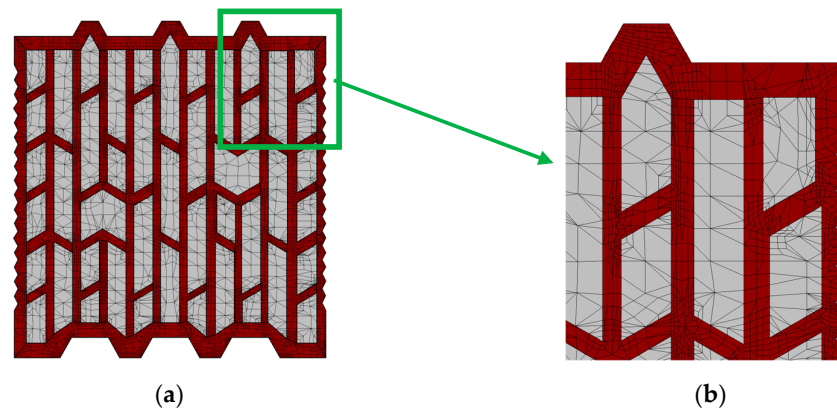
Figure 6. Schematic of the computational grid used for the brick with horizontal holes (**a**) in the ceramic products (**b**) around the air hole.

Masonry Built Performance

To calculate the thermal performance of a masonry wall, the overall heat transfer coefficient (U) must be determined. This can be achieved by considering the thermal resistances of the external surface, internal surface, plaster layer, and brick layer. The external surface resistance (R_{se}) and internal surface resistance (R_{si}) values depend on the type of wall construction and the surrounding environment. The thickness (t) and thermal conductivity (λ) of the plaster and brick layers are also necessary to calculate U. Once U is determined, it can be used to calculate the U-value of the wall, which is a measure of the rate of heat loss through the wall [30].

To further analyze the thermal performance of a masonry wall, the heat loss through the wall can be calculated using the U-value, the area of the wall, and the temperature difference between the inside and outside of the building. This information can be used to determine the energy efficiency of the building and identify areas for potential improvement. By optimizing the thickness and materials of the plaster and brick layers, as well as minimizing thermal resistances at the external and internal surfaces of the wall, the thermal performance and energy efficiency of a masonry wall can be enhanced (Table 7).

Table 7. Data and materials used in the computations.

Layer	Thickness (mm)	Thermal Conductivity (W/m·K)	Thermal Resistance (m²·K/W)
R_{si}			0.13
Plaster	20	0.87	0.023
Brick	Depends on the dimensions and the calculations through CFD of the bricks		
Plaster	20	0.87	0.023
R_{se}			0.04

Where R_{si}: refers to the thermal resistance of the interior surface of the wall, which includes all materials on the inner side of the insulation layer. This includes items such as drywall, plaster, and paint. R_{se}: refers to the thermal resistance of the exterior surface of the wall, which includes all materials on the outer side of the insulation layer. This includes items such as cladding, air cavities, and weather-resistant barriers. Plaster: A typical building material used for coating walls and ceilings.

3. Results

The outcomes of the study were segregated into two distinct sectors. Firstly, the results pertaining to the density of the fired clay samples derived from the developed mixtures were compiled. In accordance with EN1745, the thermal coefficient of the fired clay was then calculated. Secondly, the Computational Fluid Dynamics (CFD) software was utilized to estimate the thermal properties of the two brick designs, namely the horizontal hole brick and the new entry vertical perforated brick. Furthermore, based on the CFD results, the thermal performance of a building wall constructed using the computed bricks was assessed.

3.1. Laboratory Measurements of Fired Mixtures

A series of experimental tests, including preparation, extrusion, drying, and firing, was conducted to investigate the density and thermal coefficient variations of three constructed mixtures: TZ clay and TZ clay with paper sludge (labeled as TPS2 and TPS8). The results of the experimental tests are presented in Table 8, and abbreviations were used to distinguish between the samples.

Table 8. Mixture proportions and gathered results.

Parameters	Unit	TZ Mixture	TPS2 Mixture	TPS8 Mixture
Peak firing temperature	°C	900	900	900
Body density	Kg/m^3	1720	1663	1490
Thermal coefficient	W/m·K	0.52	0.49	0.43

3.2. Thermal Performance of Bricks

In Figures 7 and 8, the temperature distribution and the isothermal contours are portrayed for the brick products. The maximum temperature (20 °C) in the right-side wall refers to the inner boundary condition, and the lowest temperature (0 °C) refers to the left external wall.
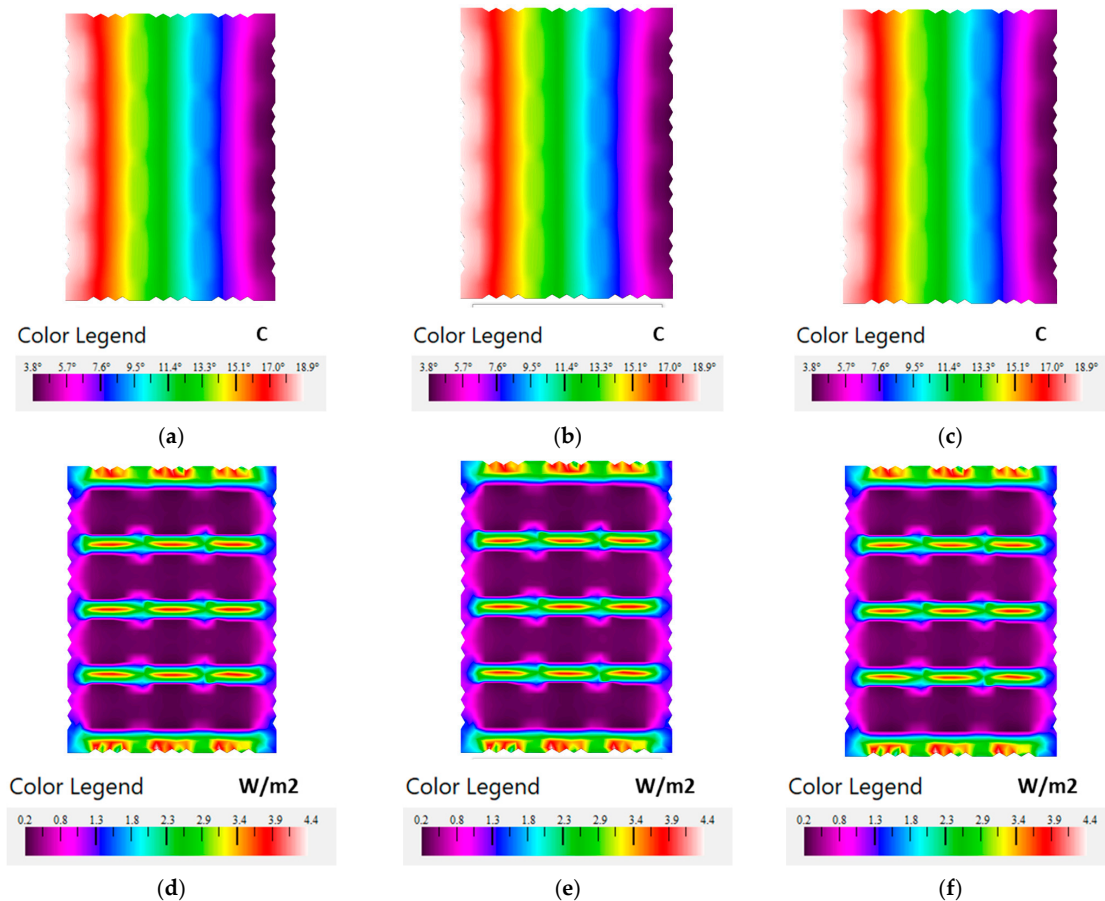

Figure 7. Hollow brick with horizontal hollows (**a**) temperature distribution in degrees Celsius constructed from TZ clay, (**b**) temperature distribution in degrees Celsius constructed from TPS2 mixture, (**c**) temperature distribution in degrees Celsius constructed from TPS8 mixture, (**d**) isothermal contour in degrees Celsius constructed from TZ clay, (**e**) isothermal contour in degrees Celsius constructed from TPS2 mixture, (**f**) isothermal contour in degrees Celsius constructed from TPS8 mixture.
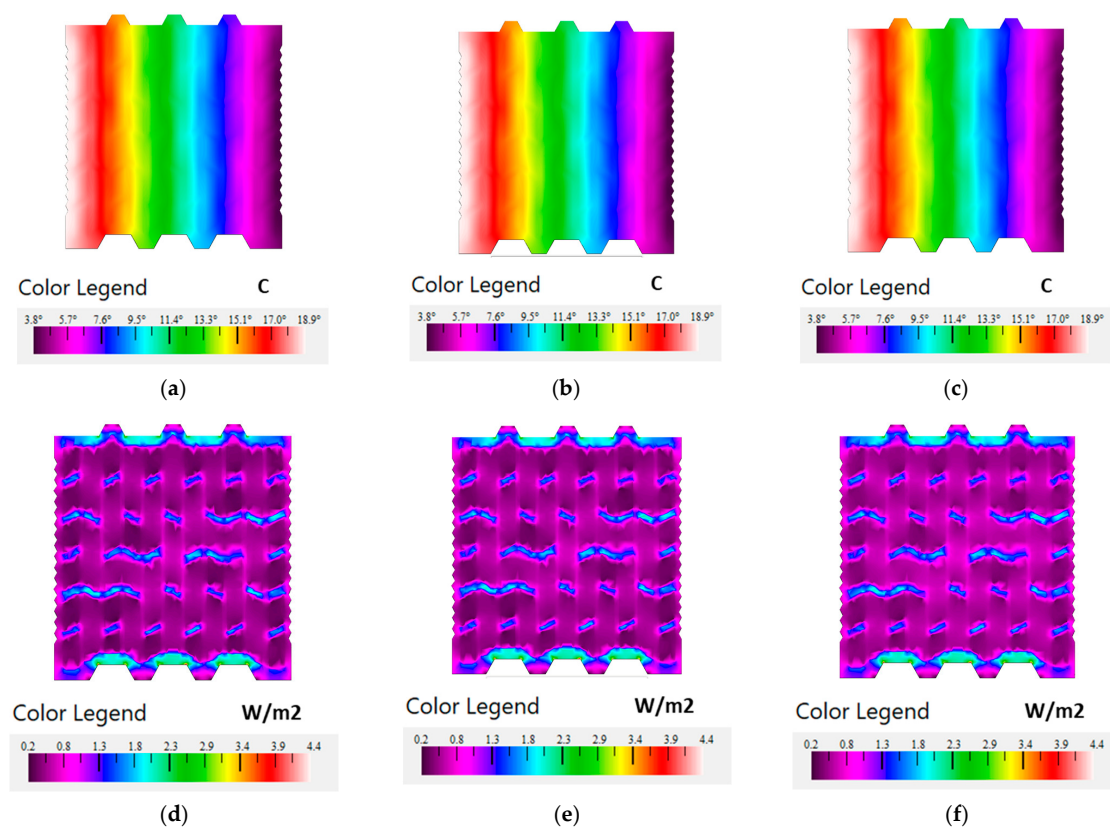
Figure 8. Vertically perforated brick (**a**) temperature distribution in degrees Celsius constructed from TZ clay, (**b**) temperature distribution in degrees Celsius constructed from TPS clay, (**c**) temperature distribution in degrees Celsius constructed from TPS8 mixture, (**d**) isothermal contour in degrees Celsius constructed from TZ clay, (**e**) isothermal contour in degrees Celsius constructed from TPS2 mixture, (**f**) isothermal contour in degrees Celsius constructed from TPS8 mixture.

Based on the above calculations, the thermal insulation properties of the two (2) studied bricks are described in Table 9:

Table 9. Mixture proportions and gathered results.

| Description	Thermal Conductivity (W/m·K)	Thermal Transmittance (W/m²·K)	Thermal Resistance (m²·K/W)
Horizontal hollows brick TZ clay	0.1676	1.8628	0.5368
Horizontal hollows brick TPS2 mixture	0.1639	1.8209	0.5492
Horizontal hollows brick TPS8 mixture	0.1536	1.7074	0.5857
Vertically perforated brick TZ clay	0.1616	0.6464	1.5470
Vertically perforated brick TPS2 mixture	0.1581	0.6326	1.5809
Vertically perforated brick TPS8 mixture	0.1488	0.5954	1.6796

Thermal Transmittance of bricks
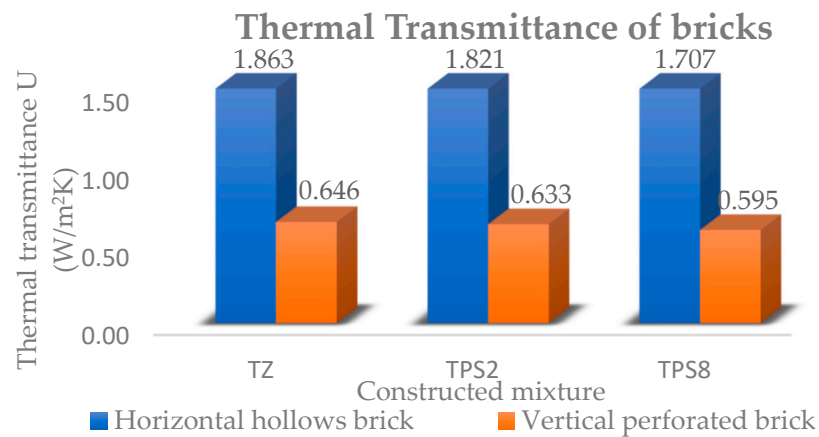
Figure 9. Thermal transmittance of the tested bricks constructed by the three tested mixtures.

3.3. Masonry-Built Performance

The thermal performance of a masonry wall is calculated using the thermal coefficient of the materials used, such as the tested clay mixtures, plaster, and the thermal resistances of the inside and outside air films (R_{si} and R_{se}). The thermal resistance of the masonry wall can be calculated by summing the thermal resistances of each layer of material, including the mortar joints. The U value of the wall can then be calculated by dividing the thermal conductivity of the wall by its thermal resistance. The U value can be used to calculate the heat loss through the wall and determine the energy efficiency of the building and the results shown above.

Table 10. Masonry-built performance for horizontal hollow brick constructed from TZ clay.

Layer	Thickness (mm)	Thermal Conductivity (W/m·K)	Thermal Resistance (m²·K/W)
R_{si}			0.13
Plaster	20	0.87	0.023
Horizontal holes brick	90	0.17	0.54
Plaster	20	0.87	0.023
R_{se}			0.04
Total resistance:		0.75	m²·K/W
U-Value		1.33	W/m²·K

Table 11. Masonry-built performance for horizontal hollow brick constructed from TPS2 mixture.

Layer	Thickness (mm)	Thermal Conductivity (W/m·K)	Thermal Resistance (m²·K/W)
R_{si}			0.13
Plaster	20	0.87	0.023
Horizontal holes brick	90	0.16	0.55
Plaster	20	0.87	0.023
R_{se}			0.04
Total resistance:		0.77	m²·K/W
U-Value		1.30	W/m²·K

Table 12. Masonry-built performance for horizontal hollow brick constructed from TPS8 mixture.

Layer	Thickness (mm)	Thermal Conductivity (W/m·K)	Thermal Resistance (m²·K/W)
R_{si}			0.13
Plaster	20	0.87	0.023
Horizontal holes brick	90	0.15	0.59
Plaster	20	0.87	0.023
R_{se}			0.04
Total resistance:		0.80	m²·K/W
U-Value		1.25	W/m²·K

Table 13. Masonry-built performance for vertically perforated brick constructed from TZ mixture.

Layer	Thickness (mm)	Thermal Conductivity (W/m·K)	Thermal Resistance (m²·K/W)
R_{si}			0.13
Plaster	20	0.87	0.023
Horizontal holes brick	250	0.16	1.55
Plaster	20	0.87	0.023
R_{se}			0.04
Total resistance:		1.76	m²·K/W
U-Value		0.57	W/m²·K

Table 14. Masonry-built performance for vertically perforated brick constructed from TPS2 mixture.

Layer	Thickness (mm)	Thermal Conductivity (W/m·K)	Thermal Resistance (m²·K/W)
R_{si}			0.13
Plaster	20	0.87	0.023
Horizontal holes brick	250	0.16	1.58
Plaster	20	0.87	0.023
R_{se}			0.04
Total resistance:		1.80	m²·K/W
U-Value		0.56	W/m²·K

Table 15. Masonry-built performance for vertically perforated brick constructed from TPS8 mixture.

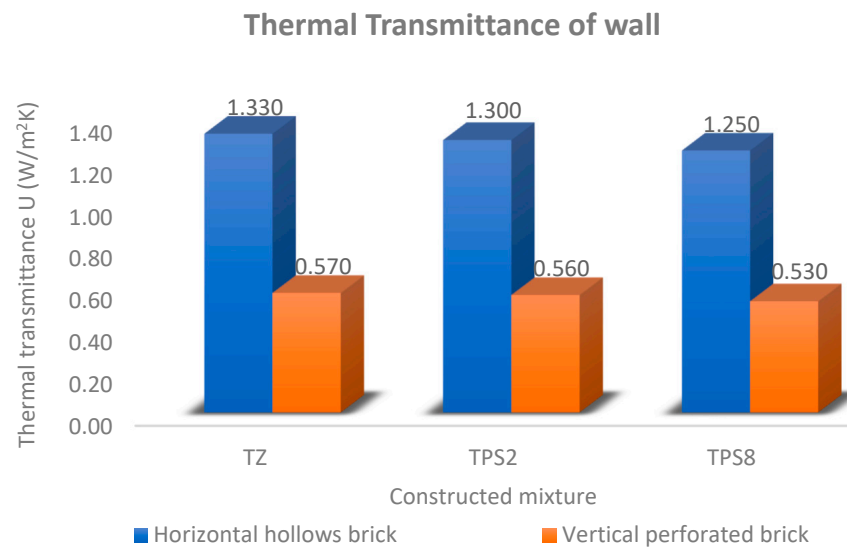| Layer	Thickness (mm)	Thermal Conductivity (W/m·K)	Thermal Resistance (m²·K/W)
R_{si}			0.13
Plaster	20	0.87	0.023
Horizontal holes brick	250	0.15	1.68
Plaster	20	0.87	0.023
R_{se}			0.04
Total resistance:		1.90	m²·K/W
U-Value		0.53	W/m²·K

Thermal Transmittance of wall

Figure 10. Thermal transmittance of building wall constructed by the tested bricks and mixtures.

4. Discussion

The present study aimed to investigate the potential of solid waste material as an additive to reduce the density of clay-based mixtures and improve their thermal performance. Three different mixtures were prepared, one with 100% clay material, one with 98% clay material and 2% solid waste material, and another with 92% clay material and 8% solid waste material. The addition of solid waste material resulted in a maximum of 17.3% decrease in the thermal coefficient of the mixtures.

The prepared mixtures were extruded into brick samples and subjected to drying and firing at 900 °C in a pilot brick and tile industry environment. The density and thermal coefficient of the fired clay samples were measured and used to simulate the thermal performance of two different brick designs using computational fluid dynamics (CFD) software. The first design was the typical Greek brick with horizontal hollows, while the second design was a vertical perforated brick, which is a new entrant in the Greek market.

The results of the study, can be seen in Tables 10–15, showed that the geometry of the brick was a critical factor that could significantly improve the thermal insulation of a building. Additionally, reducing the density of the final product by incorporating lightweight additives into the production mixture could also play a significant role in enhancing thermal insulation. It was observed that the λ value of the fired product's clay should be the primary parameter that a brick industry should aim to achieve. Furthermore, changing the molds in vertically perforated bricks could potentially create differences in the production environment.

The incorporation of solid waste material as an additive in clay-based mixtures has shown promising results in both reducing density and enhancing thermal performance. One such waste material, paper sludge, which predominantly consists of organic components like cellulose fibers, has proven beneficial in brick production. When these bricks undergo the firing process, the organic materials within the paper sludge combust and create voids within the clay matrix. These voids serve as channels for the escape of gases, effectively preventing the formation of defects such as cracks or warping that could compromise the structural integrity of the bricks. Therefore, despite the inclusion of paper sludge, the resulting bricks maintain their mechanical strength. This combination of waste material incorporation and optimized brick geometry highlights the potential for sustainable and thermally efficient building practices, as it addresses both the disposal of solid waste and the improvement of thermal insulation in construction. Further research is needed to explore the potential of different solid waste materials as additives in the production of clay-based mixtures and their impact on the thermal performance of buildings.

5. Conclusions

Based on the results presented, it can be concluded that the addition of paper sludge to fired clay material can significantly improve the thermal insulation properties of both individual bricks and masonry walls constructed using these bricks. The use of paper sludge reduced the thermal coefficient of the fired clay material by 17%, which resulted in a reduction of the U value and an increase in the resistance (R) of the bricks and masonry walls.

When comparing the thermal insulation properties of the standard 90 cm horizontal hollow brick of the Greek market to the new entry vertically perforated brick, it was found that while the improvement in the thermal coefficient of the vertically perforated brick was only 3 to 3.5%, there was a significant improvement in the R value of the product (Figure 9), which presented 188% improvement, and a 65% better U value. Similarly, the masonry wall constructed using the vertically perforated brick showed a significant improvement of 135% in its thermal insulation properties.

It is important to note that the maximum difference range was observed between the horizontal brick without the paper sludge addition and the vertically perforated brick with the paper sludge addition. In this case, the thermal coefficient of the brick presented an 11% deviation, and the U value of the brick improved by 68%. Moreover, the U value of the masonry wall constructed using the vertically perforated brick with the paper sludge addition showed a 61% improvement.

These results suggest that the use of vertically perforated bricks with paper sludge addition could be an effective strategy for improving the thermal insulation properties of masonry walls (Figure 10). Moreover, the use of paper sludge can help reduce the environmental impact of the manufacturing process of fired clay bricks. The findings of this study could be of significant interest to the construction industry, particularly for builders and architects looking to improve the energy efficiency of buildings while also incorporating sustainable materials. However, the use of paper sludge exceeding 10% in the brick mass creates many difficulties (on the preparation of the product mixture, on the main extruder gear, on the final strength, etc.) and during the cutting process of the samples after extrusion. This is primarily due to the presence of fibers in the paper sludge. The cutting of ceramic brick products in the brick industry is performed using a metal wire, and the fibers tend to adhere to it, resulting in undesired fiber aggregates that affect the intended cutting dimensions of the wet product. This issue is particularly crucial for brick factories, as it may lead to the rejection of products that do not meet market standards.

Further research can be conducted to explore the potential benefits of using paper sludge in other construction materials and techniques.

In conclusion, this study highlights the importance of the geometry of bricks and the addition of solid waste as an additive in improving the thermal performance of clay-based mixtures. The results suggest that the use of lightweight additives and alternative materials in the production of bricks can lead to the development of more energy-efficient buildings. The findings of this study have significant implications for the construction industry and can contribute to sustainable waste management practices. Future research should focus on exploring the potential of different solid waste materials as additives in the production of clay-based mixtures and their impact on the thermal performance of buildings.

Author Contributions: Conceptualization, I.M. and K.K.; methodology, I.M. and K.K.; validation, I.M. and K.K.; formal analysis, I.M. and K.K.; investigation, I.M.; resources, I.M.; data curation, I.M. and K.K.; writing—original draft preparation, I.M.; writing—review and editing, I.M. and K.K.; supervision, I.M. All authors have read and agreed to the published version of the manuscript.

Data Availability Statement: The data presented in this study are available on request from the corresponding author.

Conflicts of Interest: The authors declare no conflict of interest.

References

1. Fernandes, F.M.; Lourenço, P.B.; Castro, F. Ancient Clay Bricks: Manufacture and Properties. In *Materials, Technologies and Practice in Historic Heritage Structures*; Dan, M.B., Přikryl, R., Török, Á., Eds.; Springer Netherlands: Dordrecht, The Netherlands, 2010; pp. 29–48. [CrossRef]

2. Vijayan, D.S.; Mohan, A.; Revathy, J.; Parthiban, D.; Varatharajan, R. Evaluation of the impact of thermal performance on various building bricks and blocks: A review. *Environ. Technol. Innov.* **2021**, *23*, 101577. [CrossRef]

3. Cuce, P.M.; Cuce, E.; Sudhakar, K. A systematic review of thermal insulation performance of hollow bricks as a function of hollow geometry. *Int. J. Ambient Energy* **2022**, *43*, 4406–4415. [CrossRef]

4. Dondi, M.; Mazzanti, F.; Principi, P.; Raimondo, M.; Zanarini, G. Thermal Conductivity of Clay Bricks. *J. Mater. Civ. Eng.* **2004**, *16*, 8–14. [CrossRef]

5. Ismaiel, M.; Chen, Y.; Cruz-Noguez, C.; Hagel, M. Thermal resistance of masonry walls: A literature review on influence factors, evaluation, and improvement. *J. Build. Phys.* **2022**, *45*, 528–567. [CrossRef]

6. Uygunoğlu, T.; Özgüven, S.; Çalış, M. Effect of plaster thickness on performance of external thermal insulation cladding systems (ETICS) in buildings. *Constr. Build. Mater.* **2016**, *122*, 496–504. [CrossRef]

7. Kizinievič, O.; Kizinievič, V.; Malaiškienė, J. Analysis of the effect of paper sludge on the properties, microstructure and frost resistance of clay bricks. *Constr. Build. Mater.* **2018**, *169*, 689–696. [CrossRef]

8. Aouba, L.; Coutand, M.; Perrin, B.; Lemercier, H. Predicting thermal performance of fired clay bricks lightened by adding organic matter: Improvement of brick geometry. *J. Build. Phys.* **2015**, *38*, 531–547. [CrossRef]

9. Muñoz, P.; Morales, M.P.; Letelier, V.; Mendívil, M.A. Fired clay bricks made by adding wastes: Assessment of the impact on physical, mechanical and thermal properties. *Constr. Build. Mater.* **2016**, *125*, 241–252. [CrossRef]

10. Meukam, P.; Noumowe, A.; Jannot, Y.; Duval, R. Caractérisation thermophysique et mécanique de briques de terre stabilisées en vue de l'isolation thermique de bâtiment. *Mater. Struct.* **2003**, *36*, 453–460. [CrossRef]

11. Antoniadis, K.D.; Assael, M.J.; Tsiglifisi, C.A.; Mylona, S.K. Improving the Design of Greek Hollow Clay Bricks. *Int. J. Thermophys.* **2012**, *33*, 2274–2290. [CrossRef]

12. Labò, S.; Marini, A. In-plane flexural behavior of hollow brick masonry walls with horizontal holes. *Eng. Struct.* **2022**, *273*, 115086. [CrossRef]

13. Lourenço, P.B.; Vasconcelos, G.; Medeiros, P.; Gouveia, J. Vertically perforated clay brick masonry for loadbearing and non-loadbearing masonry walls. *Constr. Build. Mater.* **2010**, *24*, 2317–2330. [CrossRef]

14. Lacarrière, B.; Trombe, A.; Monchoux, F. Experimental unsteady characterization of heat transfer in a multi-layer wall including air layers—Application to vertically perforated bricks. *Energy Build.* **2006**, *38*, 232–237. [CrossRef]

15. Mahmood, T.; Elliott, A. A review of secondary sludge reduction technologies for the pulp and paper industry. *Water Res.* **2006**, *40*, 2093–2112. [CrossRef]

16. Goel, G.; Kalamdhad, A.S. An investigation on use of paper mill sludge in brick manufacturing. *Constr. Build. Mater.* **2017**, *148*, 334–343. [CrossRef]

17. Cusidó, J.A.; Cremades, L.V.; Soriano, C.; Devant, M. Incorporation of paper sludge in clay brick formulation: Ten years of industrial experience. *Appl. Clay Sci.* **2015**, *108*, 191–198. [CrossRef]

18. Makrygiannis, I.; Tsetsekou, A. Efficient Recovery of Solid Waste Units as Substitutes for Raw Materials in Clay Bricks. *Recycling* **2022**, *7*, 75. [CrossRef]

19. Vieira, C.M.F.; Pinheiro, R.M.; Rodriguez, R.J.S.; Candido, V.S.; Monteiro, S.N. Clay bricks added with effluent sludge from paper industry: Technical, economical and environmental benefits. *Appl. Clay Sci.* **2016**, *132–133*, 753–759. [CrossRef]

20. Vodova, L.; Sokolar, R.; Hroudova, J. The Effect of CaO Addition on Mechanical Properties of Ceramic Tiles. *Int. J. Civ. Environ. Eng.* **2014**, *8*, 717–720.

21. Sutcu, M.; Ozturk, S.; Gencel, O. Synergic effect of recycled paper sludge and expanded perlite on the engineering properties of porous clay bricks: A new mathematical modelling approach. *Constr. Build. Mater.* **2023**, *370*, 130450. [CrossRef]

22. Amorós, J.L. *Manual para el Control de la Calidad de Materias Primas Arcillosas*; Instituto de Tecnología Cerámica-AICE: Castellón de la Plana, Spain, 1998.

23. Makrygiannis, I.; Tsetsekou, A. Effect of Expanded Perlite in the Brick Mixture on the Physicochemical and Thermal Properties of the Final Products. *J. Compos. Sci.* **2022**, *6*, 211. [CrossRef]

24. De Araújo, M.V.; Pereira, A.S.; de Oliveira, J.L.; Brandão, V.A.A.; de Brasileiro Filho, F.A.; da Silva, R.M.; de Lima, A.G.B. Industrial Ceramic Brick Drying in Oven by CFD. *Materials* **2019**, *12*, 1612. [CrossRef] [PubMed]

25. Nigay, P.M.; Cutard, T.; Nzihou, A. The impact of heat treatment on the microstructure of a clay ceramic and its thermal and mechanical properties. *Ceram. Int.* **2017**, *43*, 1747–1754. [CrossRef]

26. Makrygiannis, I.; Karalis, K. *Using Simulation to Model Thermal Properties of Clay Masonry and Wall Elements*; CFI Ceramic Forum International: Baden-Baden, Germany, 2018.

27. Karalis, K.T.; Karkalos, N.; Cheimarios, N.; Antipas, G.S.E.; Xenidis, A.; Boudouvis, A.G. A CFD analysis of slag properties, electrode shape and immersion depth effects on electric submerged arc furnace heating in ferronickel processing. *Appl. Math. Model.* **2016**, *40*, 9052–9066. [CrossRef]

28. Karalis, K.; Karalis, N.; Karkalos, N.; Antipas, G.S.E.; Xenidis, A. Computational fluid dynamics analysis of a three-dimensional electric submerged arc furnace operation. *Open Sci. Framew.* **2020**, 1–19. [CrossRef]

29. Karalis, K.; Karkalos, N.; Antipas, G.S.E.; Xenidis, A. Pragmatic analysis of the electric submerged arc furnace continuum. *R. Soc. Open Sci.* **2017**, *4*, 170313. [CrossRef]

30. Feist, D.W. *Certification Criteria for EnerPHit Insulation Systems*; Passivhaus Institute: Darmstadt, Germany, 2012.